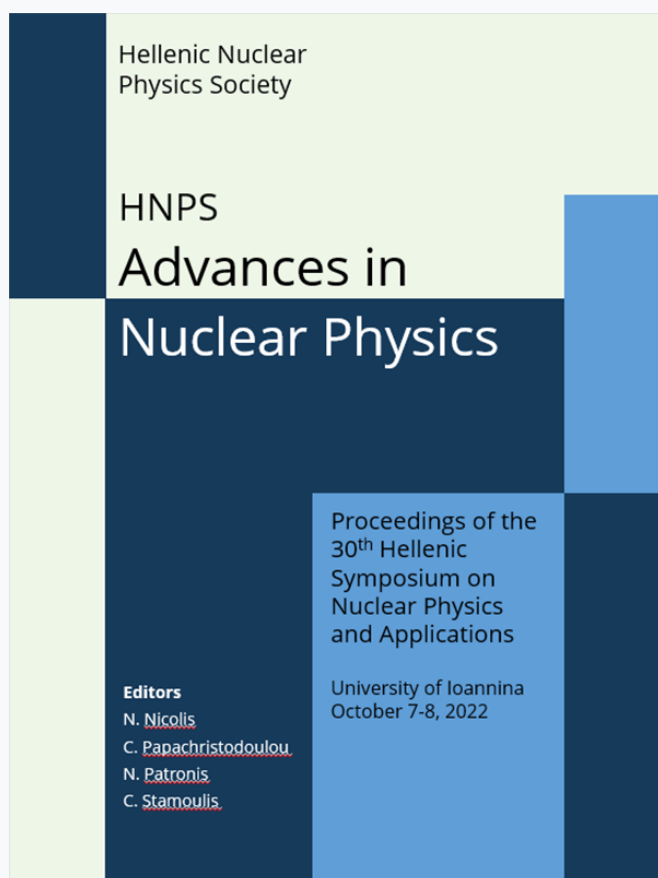


HNPS Advances in Nuclear Physics

Vol 29 (2023)

HNPS2022



Neutron Flux Determination for the NEAR Station at the CERN n_TOF Facility Using the SAND II Unfolding Code

Christoforos Frantzis, Roza Vlastou, Micheal Kokkoris, Maria Diakaki, Veatriki Michalopoulou, Sotiris Chasapoglou, Sotirios Alexandros Kopanos, Stylianos Stoulos, Pavlos Koseoglou

doi: [10.12681/hnpsanp.5185](https://doi.org/10.12681/hnpsanp.5185)

Copyright © 2023, Christoforos Frantzis, Roza Vlastou, Micheal Kokkoris, Maria Diakaki, Veatriki Michalopoulou, Sotiris Chasapoglou, Sotirios Alexandros Kopanos, Stylianos Stoulos, Pavlos Koseoglou



This work is licensed under a [Creative Commons Attribution-NonCommercial-NoDerivatives 4.0](https://creativecommons.org/licenses/by-nc-nd/4.0/).

To cite this article:

Frantzis, C., Vlastou, R., Kokkoris, M., Diakaki, M., Michalopoulou, V., Chasapoglou, S., Kopanos, S. A., Stoulos, S., & Koseoglou, P. (2023). Neutron Flux Determination for the NEAR Station at the CERN n_TOF Facility Using the SAND II Unfolding Code. *HNPS Advances in Nuclear Physics*, 29, 176–182. <https://doi.org/10.12681/hnpsanp.5185>

Neutron Flux Determination for the NEAR Station at the CERN n_TOF Facility Using the SAND II Unfolding Code

C. Frantzis^{1,*}, R. Vlastou¹, M. Kokkoris¹, M. Diakaki¹, V. Michalopoulou¹, S. Chasapoglou¹,
S.A. Kopanos¹, S. Stoulos², P. Koseoglou³

¹ Department of Physics, National Technical University of Athens, 157 80 Athens, Greece

² Department of Physics, Aristotle University of Thessaloniki, Thessaloniki, Greece

³ Institut für Kernphysik, Technische Universität zu Darmstadt, Darmstadt, Germany

Abstract The NEAR station, a new experimental area of the n_TOF facility, was established after the second long shut down of CERN in 2020. This new area was created in order to exploit *in situ* the high instantaneous neutron flux (originating from proton spallation into a lead target in bunches with momenta reaching up to 20 GeV/c). The reason for the creation of the NEAR station is to utilize the neutrons for experiments related to radiation damage on materials and nuclear astrophysics and the corresponding neutron flux was characterized via extensive neutron multiple foil activation measurements. The irradiated foils were subsequently measured using high purity germanium detectors (HPGe) to determine their induced activities. Finally, the widely used SAND II unfolding code was implemented for the characterization of the neutron flux, using the evaluated cross sections from the IRDFF library, along with the experimentally derived activities. The preliminary results concerning the neutron flux determined in the present work are compared with the corresponding FLUKA simulated ones.

Keywords SAND II, multiple-foil activation, neutron flux

INTRODUCTION

After the second long CERN shutdown for upgrade purposes [1, 2], a new experimental area at the n_ToF facility has been installed to investigate material radiation strength phenomena and reactions relevant to Nuclear Astrophysics by irradiation and activation of short-lived radioactive isotopes or small mass targets [3]. Unlike the experimental areas EAR1 and EAR2, located at ~185 m and ~20 m, respectively from the lead spallation target [4, 5], the new experimental area, called “NEAR station”, is only 3 meters away and thus exploits the high neutron flux that the facility provides from the thermal region up to a few GeV [6, 7]. For this intense flux level and short neutron flight path, none of the time-of-flight active detectors can provide the required neutron energy resolution, thus in this case, the multiple foil activation technique was deemed much more suitable for the characterization of the neutron flux.

Following the foil irradiation that was performed between the 28th of September and the 20th of October 2021 and the corresponding spectrum analysis, the unfolding SAND II code was implemented for the determination of the neutron flux, in the energy range between 10⁻¹⁰ and 18 MeV [8]. The code uses the experimentally measured reaction saturated activities from the irradiated foils, yielding the necessary information for the flux characterization, within the energy range of each threshold and capture nuclear reaction. In addition, accurate group cross sections for each reaction and for each SAND II energy interval were implemented in the code. The IRDFF library, which provides group cross sections suitable for the aforementioned code, was ideal for this purpose. It must be noted that all the relevant correction factors,

* Corresponding author: christoforosfrantzis@gmail.com

related to the self-absorption of gamma-rays and the self-shielding of neutrons in the samples, were obtained from MCNP simulations [9].

EXPERIMENTAL PROCEDURE

ACTIVATION

The neutron flux characterization, was based on the experimental foil saturated activities, following the foil irradiation, using the equation:

$$\Phi \cdot \sigma_i \cdot N = SA_i = \frac{N_\gamma}{I_\gamma \cdot \varepsilon \cdot (1 - e^{-\lambda t_m}) \cdot e^{-\lambda t_w} \cdot t_{irr} \cdot f_c \cdot f_M \cdot f_s}, \quad (1)$$

where N_γ is the yield obtained from the HPGe detector, I_γ is the gamma ray intensity of the corresponding isotope created from each induced neutron reaction, t_m is the yield acquisition time, t_w is the time between the end of irradiation and the start of the gamma ray spectrum acquisition, t_{irr} is the irradiation time, ε is the HPGe detector absolute peak efficiency with respect to each gamma ray energy, f_c is a correction factor related to the neutron beam fluctuations and f_M , f_s are correction factors concerning the gamma ray self-absorption within the irradiated foil and the relative difference of the solid angle subtended by the foil relative to the corresponding one subtended by the point source used for the determination of the detector efficiency respectively.

The experimental saturated activities combined with the evaluated group cross-sections, which will be discussed in the following sections, are essential for the accurate determination of the neutron flux.

FOIL USED & CROSS SECTIONS

The variety of isotopes used, and their induced activities covered a quite broad neutron energy range but due to the SAND II program energy interval limitations, only the reactions that occurred within the energy range between 0 – 18 MeV were used and will be showed in this paper (Fig. 1).

It should be noted here that the foil dimensions (Table 1) were selected based on their reaction cross section values and their half-lives.

Table 1. Foil materials used with respect to their physical properties, such as thickness, mass, and diameter.

Sample	Thickness [mm]	Diameter [mm]	Mass [g]	Sample	Thickness [mm]	Diameter [mm]	Mass [g]
In	0.5	13	0.4675±0.002	Au3	0.1	3	0.0142±0.0003
Sc	0.3	3	0.0073±0.0001	Au4	0.1	3	0.0149±0.0003
W	0.5	12.7	1.2349±0.0001	Au5	0.1	3	0.0148±0.0002
Bi	1	13	1.1070±0.0003	Au6	0.025	13	0.0550±0.0002
Cd	1	12.7	1.0714±0.0002	Co	0.5	3	0.0348±0.0001
Au1	0.5	3	0.0709±0.0002	Al	0.45-0.55	13	0.1694±0.0003
Au2	0.5	3	0.0712±0.0003	Ni	0.5	13	0.5624±0.0001

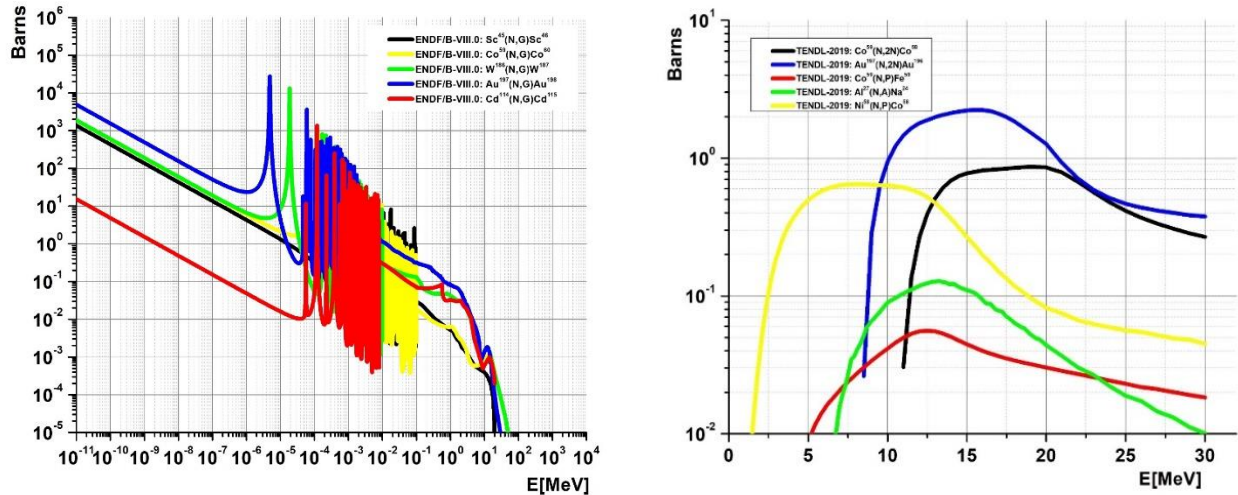


Figure 1. The induced reaction cross sections related to the foil saturated activities and the SAND II code energy range limitations.

DATA ANALYSIS

γ -RAY SPECTROSCOPY

Following the irradiation, the foil activities were determined via gamma-ray spectroscopy, implementing HPGe detectors of 80% relative efficiency at distances around ~9 cm, ~12 cm and ~15 cm from the detector window. At such distances the contribution related to the true coincidence summing effect was negligible. A ¹⁵²Eu point source was used for the energy calibration of the spectra and the determination of the absolute peak efficiency (ϵ) of the detector. The obtained experimental data were subsequently fitted using the widely used IAEA function:

$$\epsilon(E) = A + \frac{B}{E} + \frac{C}{E^2} + \frac{D}{E^3} \quad (2)$$

All the gamma-ray spectra were analyzed using the SPECTRW code [10].

CALCULATED ACTIVITIES

The neutron induced activities were calculated utilizing information related to the energy of the impinging neutrons. It should be noted here that correction factors which were related to the self-absorption, self-shielding, and neutron scattering effects were estimated using MCNP5 Monte-Carlo simulations.

THRESHOLD ACTIVITIES CORRECTION FACTOR

The threshold saturated activities (Table 2) had to be modified in order to correspond to the specific portion of the neutron flux within the energy range between 0 and 18 MeV. This correction factor was crucial in order to obtain an accurate estimation of the flux in the fast energy neutron region. For calculation purposes, the FLUKA simulation code was utilized following the equations:

$$\text{From } 10 - 50 \text{ [MeV]: } A_1 = \sum \sigma_i \cdot \Phi_i \cdot (E_{i+1} - E_i) \quad (3)$$

$$\text{From } 10 - 18 \text{ [MeV]: } A_2 = \sum \sigma_i \cdot \Phi_i \cdot (E_{i+1} - E_i) \quad (4)$$

$$\frac{A_1}{A_2} \cdot A_{measured} = A_{SAND II input}$$

where A corresponds to the threshold saturated activities, $E_{i+1} - E_i$ is the energy interval with respect to the neutron flux Φ_i , and the quantity σ_i is the reaction cross section.

Table 2. Calculated saturated activities that correspond to the neutron energy range of 0 – 18 MeV. Different foils were placed for irradiation at different positions, and thus some of them had other foils as covers.

Sample	Reaction	Saturated Activity [Bq/TN]	Sample	Reaction	Saturated Activity [Bq/TN]
Au1	(n, γ)	2.994515E-16	Au6	(n, γ)	7.189139E-16
	(n,2n)	4.509165E-18		(n,2n)	3.974748E-18
Au2	(n, γ)	2.741176E-16	Cd-114	(n, γ)	1.432550E-17
	(n,2n)	4.343933E-18	Sc-45	(n, γ)	4.425686E-17
Au3	(n, γ)	2.785879E-16	Ni-58	(n,p)	4.036337E-18
	(n,2n)	4.047516E-18	W-186	(n,p)	1.852110E-16
Au4	(n, γ)	5.039652E-16	Co-59	(n, γ)	7.217969E-17
	(n,2n)	3.962416E-18		(n,2n)	1.893099E-18
Au5	(n, γ)	4.678819E-16		(n,p)	2.707480E-19
	(n,2n)	4.031398E-18	Al-27	(n, α)	2.989190E-19

SAND II UNFOLDING CODE

SAND II BASIC ALGORITHM

The SAND II (Spectrum Analysis by Neutron Detectors II) unfolding code has been developed to determine spectra by a fully automated iterative method when a multiple foil activation technique has been implemented. The code uses as input the already experimentally derived neutron induced activities, an initial differential neutron flux ('guess' spectrum) and the grouped cross sections from the IRDF library, which creates the latter cross sections especially for the named code. The SAND II algorithm subsequently adjusts iteratively the neutron flux spectrum to obtain an appropriate fit between the theoretically calculated and the experimentally determined reaction rates, within the energy range of 0-18 MeV divided into 620 intervals (621 energy points). It should be noted here that the code is very sensitive with respect to the initial user-supplied neutron flux spectrum, since the exact determination of the 620 interval values with a small number of measured activities creates a non-inverse matrix problem [see eq. 5], since each activity used as input represents an equation of 620 unknown values. In this specific work, only 13 saturated activities were used and for reliability purposes, 4 different initial 'guess' neutron flux spectra were implemented, which were closely related to the FLUKA Monte-Carlo simulation results [Fig 2].

$$\begin{bmatrix} \sigma_1^{[1]} & \cdots & \sigma_{620}^{[1]} \\ \vdots & \ddots & \vdots \\ \sigma_1^{[13]} & \cdots & \sigma_{620}^{[13]} \end{bmatrix} \begin{bmatrix} \Phi_1 \\ \vdots \\ \vdots \\ \vdots \\ \Phi_{620} \end{bmatrix} = \begin{bmatrix} A^{[1]} \\ \vdots \\ A^{[13]} \end{bmatrix} \quad (5)$$

The SAND II iterative procedure uses the following method to determine the neutron flux:

$$A_{i,j}^{[k]} = \Phi_j^{[k]} \cdot \bar{\sigma}_{i,j} \cdot (E_{j+1} - E_j) \quad (6)$$

$$A_i^{[k]} = \sum_{j=1}^m A_{i,j}^{[k]} \quad (7)$$

$$W_{i,j}^{[k]} = \frac{\sum_{l(l_1+1)}^{l_2} A_{i,l}^{[k]}}{(l_2-l_1+1)A_i^{[k]}} \tag{8}$$

$$C_j^{[k]} = \frac{\sum_{i=1}^n W_{i,j}^{[k]} \cdot \ln(A_i/A_i^{[k]})}{\sum_{i=1}^n W_{i,j}^{[k]}} \tag{9}$$

$$\Phi_j^{[k+1]} = \Phi_j^{[k]} e^{C_j^{[k]}} \tag{10}$$

SMOOTHING FACTOR N_s

As mentioned above, the determination of 620 intervals using only 13 equations is a rather difficult task considering the limitations of the neutron-induced reactions. Thus, except from carefully chosen initial neutron spectra, a moving linear averaging factor was adopted by means of the parameter N_s , which contributes to the weight factor [eq. 8] where the interval l_1 to l_2 is shown, includes the points which are specified by the value of the smoothing factor N_s . This technique helped us solve the aforementioned system of 13 equations with 620 unknown values and reach a satisfactory convergence between the 4 different initial fluxes. The moving linear averaging factor is biasing the solution of a specific flux interval [eq. 9, 10] by considering not only the cross-section shape, but also taking into account the dominant reaction.

The smoothing factor $N_s = 20$ was found to be the most reliable one among all the others, due to the clear solution convergence we have managed to achieve between the 4 different differential flux results within the energy range where most of the saturated activities contributed [Figs. 3-5].

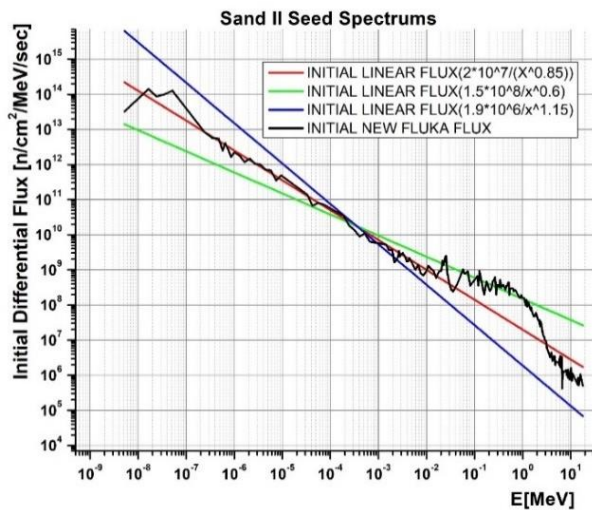


Figure 2. Representation of the 4 different initial differential neutron fluxes

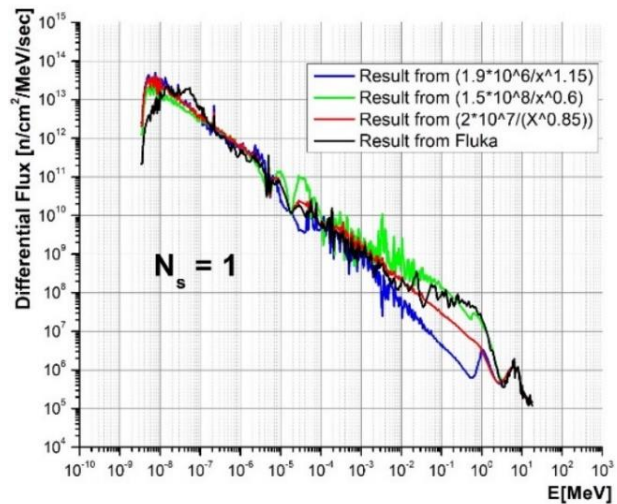


Figure 3. Results obtained using a moving linear averaging factor $N_s=1$. Artificial neutron flux resonances are visible due to the non-inverse matrix problem.

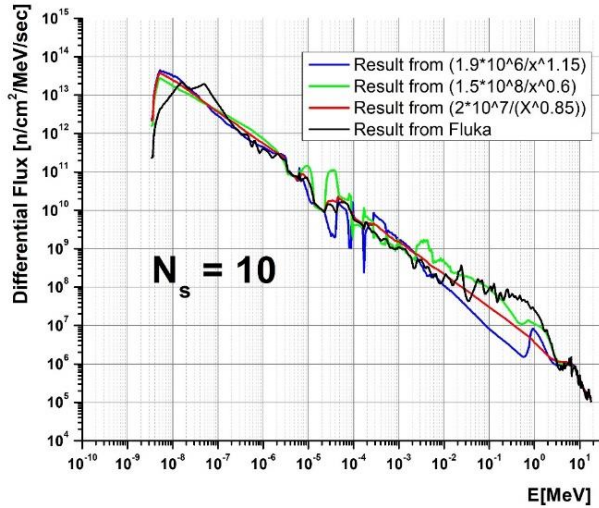


Figure 4. Results obtained using a moving linear averaging factor $N_s=10$.

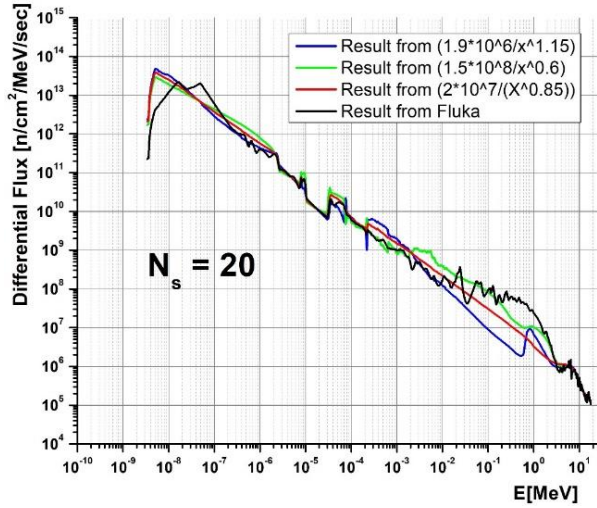


Figure 5. Results obtained using a moving linear averaging factor $N_s=20$.

RESULTS AND FUTURE PERSPECTIVES

The results presented in this paper are preliminary, as more reliable MCNP 5 simulations with high statistics are ongoing in order to provide more accurate correction factors concerning the neutron scattering and self-shielding effects incorporated especially in the gold material foils [see Table 3]. The resulted spectra presented [Fig. 6, 7] provide a very good estimation of the realistic neutron flux, as the code calculated saturated activities are within a total standard deviation of 9.46%.

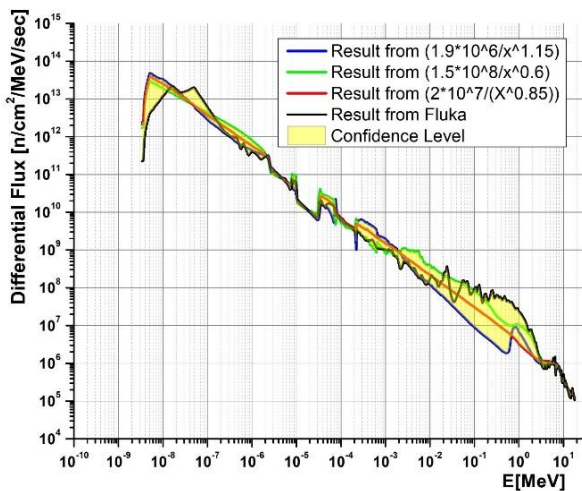


Figure 6. The clear convergence in the thermal and fast neutron energy region is attributed to the information that corresponded to the threshold and capture reactions.

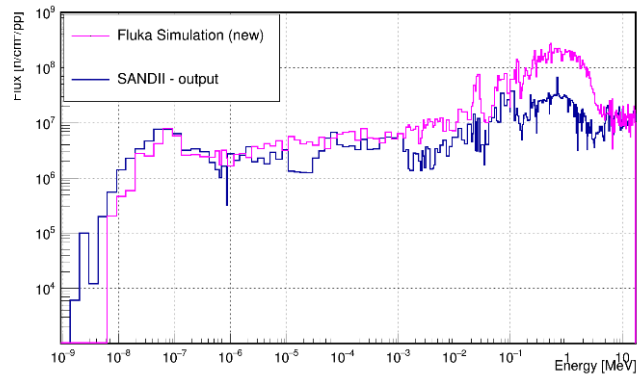


Figure 7. The preliminary SAND-II results were compared with the FLUKA simulations after adjusting the energy interval bins.

Table 3. Saturated activities (SA) obtained from the SAND II code with the corresponding deviation.

Sample	Reaction	SA [Bq/TN] Measured	SA [Bq/TN] Calculated	Deviation of Measured to Calculated SA (%)
Au-1	(n,g)	2.995×10^{-16}	3.508×10^{-16}	-14.63
Au-5	(n,g)	4.679×10^{-16}	5.262×10^{-16}	-11.08
Au-3	(n,g)	2.786×10^{-16}	2.326×10^{-16}	19.79
Au-6	(n,g)	7.189×10^{-16}	6.509×10^{-16}	10.45
Au-1	(n,2n)	2.958×10^{-18}	3.227×10^{-18}	-8.35
Sc	(n,g)	4.426×10^{-17}	4.426×10^{-17}	-0.25
Co	(n,g)	7.218×10^{-17}	7.378×10^{-17}	-2.17
Co	(n,2n)	7.307×10^{-19}	7.140×10^{-19}	2.35
Co	(n,p)	1.836×10^{-19}	1.652×10^{-19}	11.14
W	(n,g)	1.836×10^{-16}	1.860×10^{-16}	-0.42
Ni	(n,p)	3.871×10^{-18}	4.100×10^{-18}	-5.60
Al	(n,a)	2.610×10^{-19}	2.627×10^{-19}	-0.68
Cd-114	(n,g)	1.433×10^{-17}	1.441×10^{-17}	-0.56

In Fig. 7 a clear underestimation of the SAND-II neutron flux with respect to the FLUKA simulations can be observed, roughly within the energy region of $10^{-3} - 8$ MeV. The latter result obtained can be attributed to the low cross sections of the threshold reactions we have used within that specific energy interval [Fig.1]. However, a good estimation of the flux for the low neutron energies was obtained since a lot of capture reactions were used. A better estimation would be feasible after utilizing the more reliable high statistic MCNP5 simulations concerning the capture activities' correction factors, especially in the case of gold foils.

Thus, in order to finalize the results, the neutron flux values determined via the SAND-II code are to be compared with the estimations of other research teams of the n_TOF collaboration, using different approaches.

References

- [1] R. Esposito and M. Calviani. J. Neutron Res. 22, 221 (2020)
- [2] R. Esposito *et al.*, Phys. Rev. Accel. Beams 24, 093001 (2021), doi: 10.1103/PhysRevAccelBeams.24.093001
- [3] G. Gervino *et al.*, Universe 8, 255 (2022), doi.org/10.3390/universe8050255
- [4] n TOF CERN, website: <https://ntof-exp.web.cern.ch/>
- [5] C. Guerrero *et al.*, Eur. Phys. J. A 49, 27 (2013), doi:10.1140/epja/i2013-13027-6. 400 2
- [6] The nTOF Collaboration. The new nTOF NEAR Station. CERN INTC-2020-073 / INTC-I-222, 2020. Letter of Intent to the ISOLDE and Neutron Time-of-Flight Committee, European Organisation for Nuclear Research (CERN) Geneva, Switzerland, url: <https://cds.cern.ch/record/2737308/files/INTC-I-222.pdf>.
- [7] M. Ferrari *et al.*, Phys. Rev. Accel. Beams 25, 103001 (2022), doi: 10.1103/PhysRevAccelBeams.25.103001
- [8] S. Berg and W. N. McElroy. A Computer-Automated Iterative Method for Neutron Flux Spectra Determination by Foil Activation, Atomic International Tech Report AFWL-TR-67-41: CA, 1976
- [9] X-5 Monte Carlo team, MCNP-A General Monte Carlo N-Particle Transport Code, version 5, Volume I-III, LAUR-03-1987, LA-CP-03 0245 and LA-CP-03-0284 (April 2003)
- [10] C. A. Kalfas, M. Axiotis, C. Tsabaris, Nucl. Instr. and Meth. A830, 265-274 (2016)